Electronic Supplementary Information

Evaluation of Electric Double Layer Capacitors Composed of Electrode Materials Using a Gel State Derived from a Polymer Hydrogelator in the Device Fabrication Process

Mai Hirukawa [a] and Yutaka Ohsedo [b]*

[a] *Graduate School of Human Centered Engineering, Nara Women's University, Japan*

[b] *Division of Engineering, Faculty of Engineering, Nara Women's University, Kitauoyahigashi-machi, Nara 630-8506, Japan. E-mail: ohsedo@cc.nara-wu.ac.jp*

1. Figures

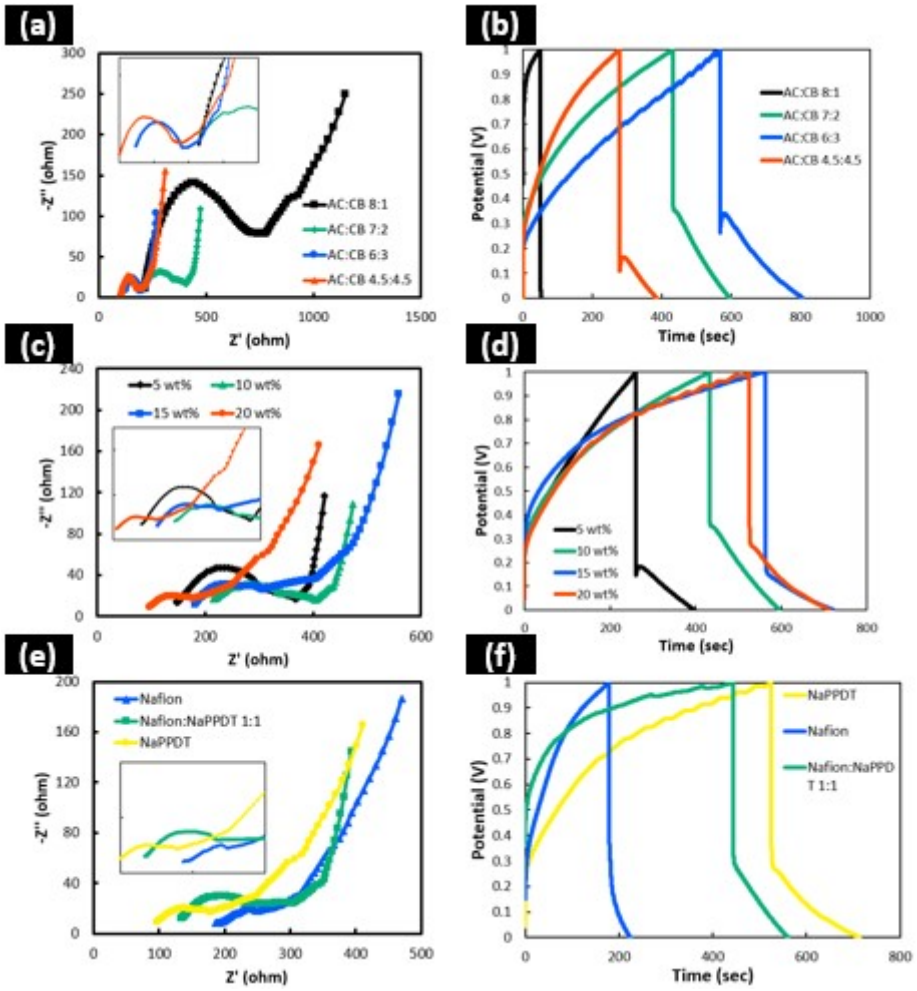

Fig. S1 Electrochemical measurements to determine the optimal material composite ratio and comparison by binder form. (a) EIS and (b) GCD graphs of samples with different carbon material composite ratios. (c) EIS and (d) GCD graphs of samples with different binder material concentrations. (e)EIS, (f) GCD graphs of different binder samples made under optimal composite conditions.

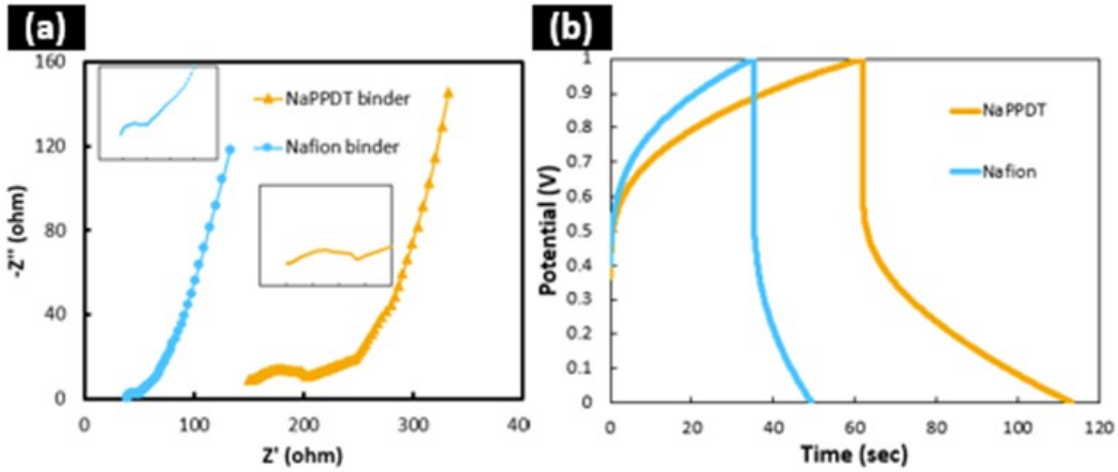

Fig. S2 Electrochemical measurements with optimal material composite ratio electrode materials dried at higher temperatures. (a) EIS, (b) GCD graph.

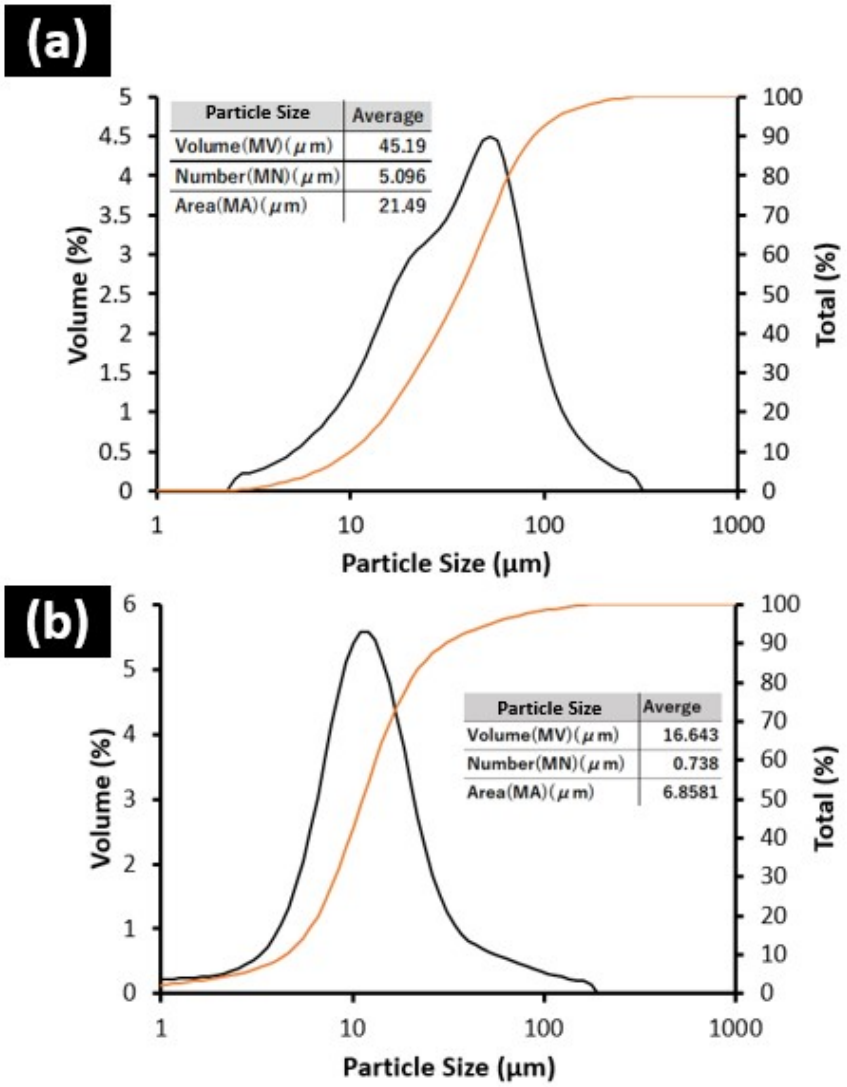

Fig. S3 Particle size distribution of (a) activated carbon and (b) carbon black used in the experiment.

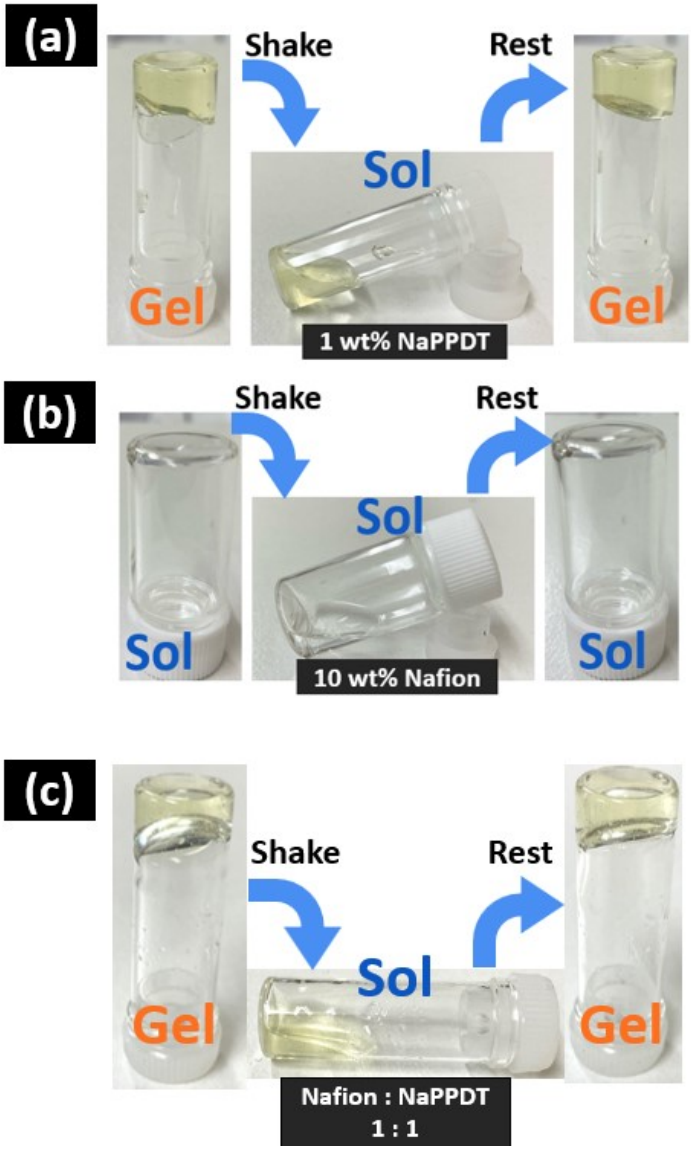

Fig. S4 Performed vial inversion of (a) 1 wt% **NaPPDT** solution (hydrogel), (b) 10 wt% Nafion solution, (c) Nafion : **NaPPDT** 1 : 1 composite material.

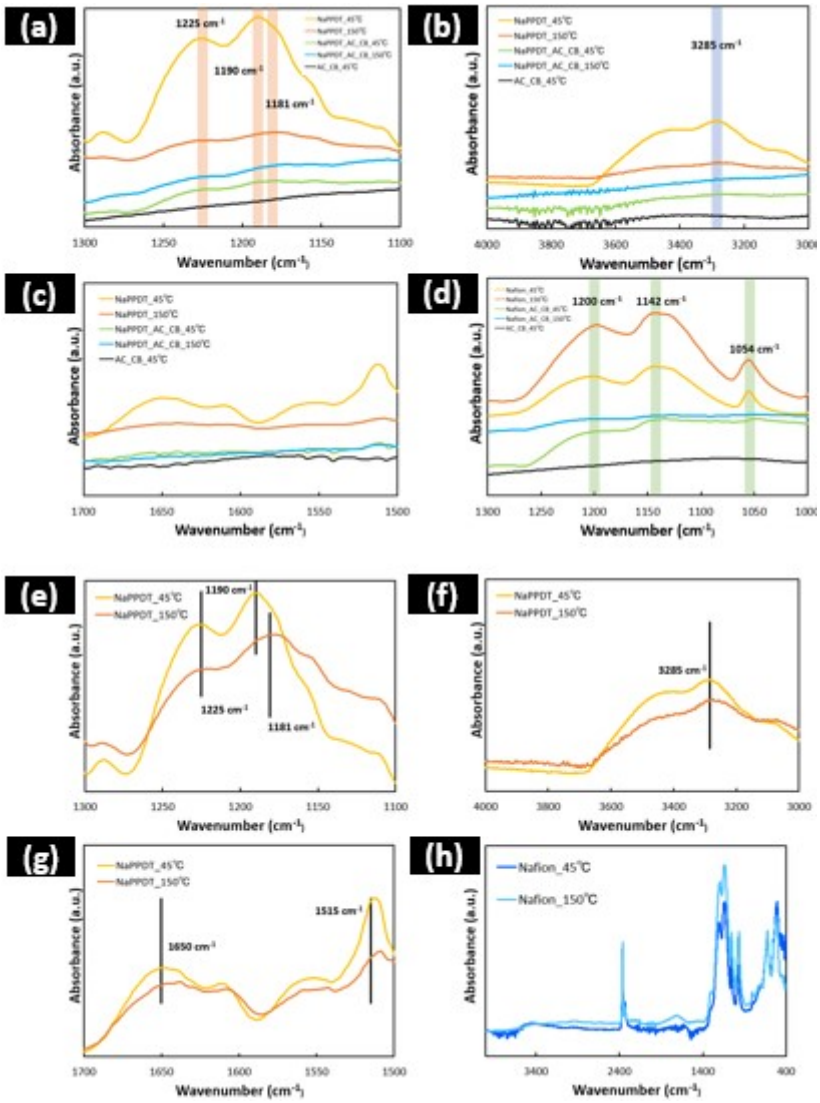

Fig. S5 Graph of ATR-FTIR measurements of composite materials. (a) Peaks associated with sulfonyl groups in the data for the **NaPPDT** composite. (b) Peaks associated with N-H stretching in the data for the **NaPPDT** composite. (c) Peak related to amide in the **NaPPDT** composite data. (d) Peaks related to sulfonic acid, in the Nafion composite data. (e) Peaks related to sulfonyl groups in the data for **NaPPDT** dried at different temperatures. (f) Peaks related to N-H stretching/contraction in the data for **NaPPDT** dried at different temperatures. (g) Peaks related to amides in the data for **NaPPDT** dried at different temperatures. (h) Overall view of the data for "Nafion" dried at different temperatures.

It was believed that elucidating the material properties of electrode materials with varying binder compositions would lead to identifying the causes of the electrochemical behaviour discussed in the previous section. Therefore, ATR-FTIR measurements were conducted to examine the

structural changes of the binder complexed with carbon particles. In the case of **NaPPDT**, shifts in the sulfonyl group (1181, 1225 cm^{-1}) and N-H stretching region (3285, 3413 cm^{-1}) have already been reported due to the incorporation of functional materials.[1] It was also anticipated that heating might induce changes in the amide group. However, no such shifts were observed in any of the samples, whether dried at 45°C or 150°C, that were complexed with AC and CB (Fig. S5a-c, ESI†). Additionally, for Nafion, it is known that there are strong signals at 1200 cm^{-1} and 1142 cm^{-1}, and a moderate absorption band around 1054 cm^{-1}, which corresponds to the symmetric stretching of the sulfonic acid group.[2] However, in this case, no significant shifts were observed at the characteristic wavelengths either (Fig. S5d, ESI†). Therefore, it is concluded that there is no interaction with the complexed carbon powder in all the binder samples and that the binder and carbon powder coexist without interfering with each other's structures.

Next, the peaks of the binders with different drying temperatures were further enlarged and compared. In the region corresponding to the sulfonyl stretch of NaPPDT, no shift was observed at 1225 cm^{-1}, whereas the low-temperature **NaPPDT** showed a peak at 1190 cm^{-1}. After high-temperature treatment, the peak shifted to a lower wavelength (1181 cm^{-1}) (Fig. S5e, ESI†). Previous studies have confirmed a shift from 1181 cm^{-1} to 1190 cm^{-1} due to the incorporation of functional particles. This result suggests that the inter-molecular interactions of the sulfonyl group in **NaPPDT** may have changed upon 150°C treatment, but this could not be fully elucidated. Next, the peaks corresponding to the N-H stretch showed no clear shift (Fig. S5f, ESI†). As for the peaks related to the amide group, focusing on the peaks at 1650 cm^{-1} and 1515 cm^{-1}, both were slightly shifted to a lower wavelength in the high-temperature treated samples, but macroscopically, there was almost no change (Fig. S5g, ESI†). Furthermore, no shifts in the peaks were observed for Nafion, confirming its resistance and stability against high-temperature heating (Fig. S5h, ESI†).

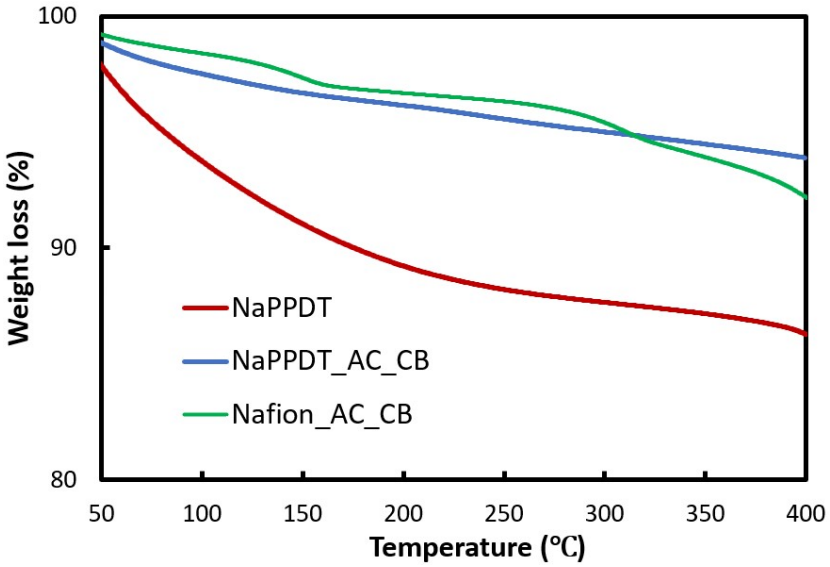

Fig. S6 Thermogravimetry analysis (TGA) of the electrode materials composed of NaPPDT and Nafion.

Thermogravimetric analysis (TGA) results of NaPPDT solid, as well as electrode materials composed of NaPPDT with AC:CB (at a ratio of 7:2) and Nafion with AC:CB (at a ratio of 7:2), are shown in Fig. S6. The measurements were conducted at a heating rate of 10 °C/min. These results show that NaPPDT alone exhibits a significant weight loss due to temperature increase, but after being used as an electrode material, the weight loss is comparable to that of electrode materialized Nafion. In particular, at temperatures above 300°C, NaPPDT-based electrode material shows a reduced weight loss compared to Nafion-based electrode material. Thus, the thermal stability of NaPPDT-based electrode materials was shown to be at the Nafion level.

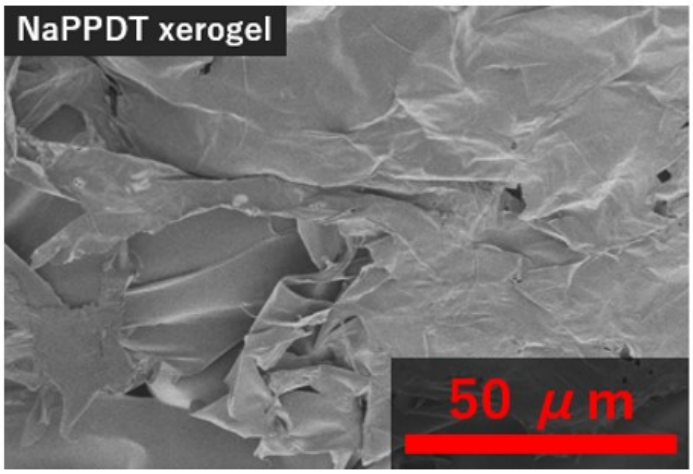

Fig. S7 Fibre structures of **NaPPDT**.

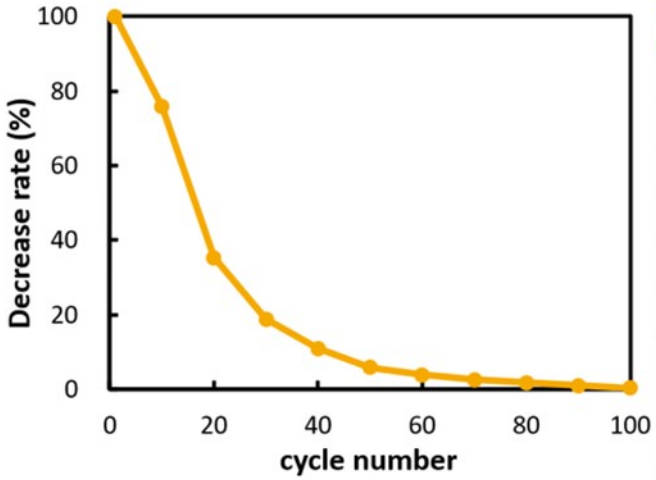

cycle	decrease rate (%)
1	100.00
10	75.75
20	35.41
30	18.89
40	10.94
50	5.87
60	3.93
70	2.69
80	1.91
90	1.05
100	0.46

Fig. S8 Cycle performance test results using **NaPPDT** binder electrode (dried at 150°C).

2. References

1 Y. Ohsedo, M. Oono, K. Saruhashi, H. Watanabe and N. Miyamoto, *Royal Society Open Science*, 2017, **4**, 171117.

2 S. Carli, M. Di Lauro, M. Bianchi, M. Murgia, A. De Salvo, M. Prato, L. Fadiga and F. Biscarini, *ACS Appl. Mater. Interfaces*, 2020, **12**, 29807–29817.